Extended rheological characterization as a tool for low-binder 3D-printing compositions

Roberto Cesar de Oliveira Romano[1], Francisco Jordão Nunes de Lima[1], José Augusto Ferreira Sales de Mesquita[1], Eduardo Maia Pan[1], Rafael Giuliano Pileggi[1]

[1] Department of Civil Construction Engineering, University of São Paulo, Brazil
rcorjau@gmail.com

Abstract. Implementing 3D-printing technology of cementitious compositions holds a significant contribution for revolutionizing the construction sector. However, the current stage of the technology often requires a higher amount of binder compared to conventional concretes, posing environmental challenges during the production of the components. So, as well as a trend in the cement industry, the development of low-binder 3D-printing compositions is an essential step for the sustainability of this process. To this strategy be successfully achieved, the impact of raw material proportioning must be studied on printing properties. Another relevant piece of information is that the development of printable compositions must be carried out in parallel with the choice of printing equipment, adapting its rheological properties to the characteristics of the printer. In this research we developed compositions with low-binder content to be used in a 1k 3D-printer, applying an extended rheological approach to understand the printability requirements. The work was started using a reference composition indicated by the equipment manufacturer, to obtain rheological information of practical interest, creating a list of parameters and behaviors for adequate printability. The development of low-binder compositions was carried out considering the concepts of packing of particles, and our target was a consumption below 290 kg/m³ of cement, the lowest reported in the literature so far for dense components. The rheological properties were investigated applying the methods of rotational rheometry, squeeze flow, Benbow and Bridgwater and flow table. With the results, was possible to highlight the significant rheological contributions at each step in the development of 3D printed compositions, improve sustainability and achieve high-quality printed structures with lower cement consumption than previously reported in the literature.

Keywords: 3D-Printing, Low-Cement Compositions, Extended Rheological Approach, Mix-design, Sustainability

1 Introduction

The introduction of 3D-printing technology for cement products has led to significant advancements in the construction sector. This innovative approach shows great promise for revolutionizing the fabrication of concrete components, providing possibilities for intricate designs without the need for molds, reducing labor costs, and enhancing construction efficiency [1]. However, a great challenge for 3D-printing development is the high binder consumption associated with processes [2], impacting significantly in environmental construction activities due to its high carbon footprint [3]. The use of limestone filler in compositions is particularly attractive due to its affordability and smaller CO_2 footprint than Port-

https://doi.org/10.24355/dbbs.084-202408160950-0

land cement, as it does not require calcination or expensive preparation [4]. However, the replacement of limestone with cement modifies the particle size distribution and surface characteristics of the concrete mix-design, resulting in changes to its rheological behavior and parameters such as yield stress and viscosity [4]. In certain instances, an excessive amount of filler can lead to increased viscosity, potentially causing difficulties in pumping and placing the concrete layer by layer [5]. So, achieving suitable rheological parameters in low-cement concrete for 3D printing presents another significant challenge [6].

In this way, the comprehension of the rheological aspects of 3D-printing cement compositions plays a vital role in determining the printability and buildability of concrete [7]. In ordinary concrete mixtures for 3D printing, adding extra cement is often employed to improve printability and ensure structural integrity [8]. However, this practice contradicts the goal of the cement industry, reduce the amount of binder consumption [9]. Therefore, alternative strategies and methodologies are needed to optimize the printability of low-cement concrete mixtures without compromising structural performance. By leveraging rheological mapping methodology, this research seeks to enhance the understanding of rheological behavior in low-cement concrete and provide valuable insights for advancing 3D printing technology in the construction industry.

2 Materials and compositions

CPV-type Portland cement, a binder equivalent to CEM I 42.5 R (European standard) or Type III (US Standard) was the only binder used in the formulations. Three limestones, originating from the same mineralogical source, but with distinct particle size distributions, and a mix of quartz sands were also selected for the study. The lend of limestones resulted in a particle size distribution with d_{50} of 15 µm and volumetric surface area of 2.4 m^2/g. The target was optimizing the particle packing. It was considered the Westman and Hugill model [10]. The consumptions of each raw material in the compositions are presented in Table 1, considering the weight, in kg, per volume of composition, in m^3. It must be clear that the air content was not considered. The reference composition (Ref Mix) is the formulation indicated by the producer of 3D-printer as a product with positive synergism between machine and printability composition. As this was the first stage of our global project for the development of eco-friendly compositions for 3D-printing, we didn't use any kind of admixture and the specimen was printed using 1k equipment. So, the main target of this part of the project was to set the rheological protocol.

Table 1. Consumption of each raw material (in kg/m^3).

Material	Ref Mix	Mix 1	Mix 2	Mix 3	Mix 4
Portland cement	639	288	288	288	288
Blend of limestone	-	674	674	517	513
Blend of sands	1422	962	962	1116	1119
Water	258	302	302	301	301

Table 2 summarize the mix-design strategy. Mix 3 was formulated to achieve optimal packing particles of both fines and coarse particles, in separate. Conversely, Mix 2 was formulated to prioritize good packing of fines, while exhibiting poorer packing of coarse particles

https://doi.org/10.24355/dbbs.084-202408160950-0

and a higher volumetric surface area. The remaining compositions were designed to exhibit intermediary physical characteristics.

Table 2. Packing of particles, according to the Westman and Hugill model, and volumetric surface area is a product of density by superficial area.

Property	Ref Mix	Mix 1	Mix 2	Mix 3	Mix 4
Total packing of particles (%)	19.5	7.45	12.3	5.61	12.3
Packing of finer particles (%)	17.2	12.9	12.9	11.5	11.6
Packing of coarse particles (%)	25.3	22.2	25.7	17.8	23.6
Volumetric surface area (m^2/cm^3)	2.17	3.28	3.36	2.67	2.78

3 Printing Parameters

The qualitative printability test was carried out using a 3D printing machine (4Constru). The printed object (Fig. 1, on the right) was modelled and sliced using the parametric modelling software Grasshopper. The modelled object was a single-walled cylinder with a diameter and total height of 300 mm. The slicing process defined a layer height of 9 mm, resulting in a layer width of 21.6 mm (Fig. 1, on the left).

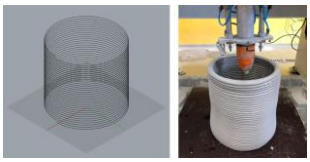

Fig. 1. Proposed design for the print test (left) and printed part (right).

The extrusion speed (spindle/rotating screw speed) was set to 2000 rpm, determined as the optimal value based on a flow rate curve developed by the research group. A circular nozzle with a diameter of 15 mm was used for the printing process. After slicing the object, the movement speed of the printing nozzle was calculated and set to 10.7 mm/s. Additionally, the printing was configured in cylindrical mode during the slicing process. The tests were conducted to visually analyse the maximum height of layer overlap.

4 Methods of testing

Mixing rheometry was performed in a Pheso rheometer (Calmetrix), using an attritor geometry of mixing placed in the planetary position of equipment. The powder was homogenized in a double-cone blender and inserted into a bowl. The total amount of water was added controlling the flow addition at 35 g/sec. The mixing stage was monitored for 240 seconds maintaining the shear speed at 180 rpm. The *shear rheometry* was performed after the mixing stage, applying the stepped flow protocol, increasing the shear speed between 30 and 350 rpm in 8 steps, and then return to 30 rpm in 7 more steps. Each step was performed by 8 seconds. Although the *flow table* test is not suitable for measuring the rheological properties of compositions for 3D printing, this test was selected because it is a standardized test used in the field of civil engineering and construction materials to assess the consistency

https://doi.org/10.24355/dbbs.084-202408160950-0

and workability of mortars. Its general procedure is outlined by the ASTM C1437/C1437M-1: Standard Test Method for Flow of Hydraulic Cement Mortar. The *Benbow and Bridgwater* method provides valuable information about the pressures and extrusion profiles of materials used in 3D printing [11]. The tests were performed in an Instron 5569 double-column universal machine with a 50 kN load cell. A metallic piston with a diameter of 51.8 mm was vertically moved at a constant speed of 1.0 mm/s, pressing the material within a fixed metallic cylinder with a diameter of 52.0 mm and a height of 157 mm. The extrusion occurred through a nozzle with a diameter of 14.8 mm at the bottom of the cylinder. The *squeeze flow* test was performed according to the specifications of Brazilian standard NBR 15839 – Rendering mortars for walls and coatings: rheological evaluation by squeeze flow, using an Instron 3345 one-column universal machine with 5 kN load cell. A sample of 101 mm diameter and 20 mm height was positioned under parallel plates and squeezed applying a displacements speed of 1.0 mm/s.

5 Results and discussion

In order to contextualize the importance of rheological evaluation in the development of the composition to be printed, it was decided to initially present the qualitative printing test performed, and the results are summarized in Table 3.

Table 3. Summary of qualitative test of printability.

Property	Ref Mix	Mix 1	Mix 2	Mix 3	Mix 4
Flowability / pumpability	Adequate	Adequate	Adequate	Adequate	Adequate
Initial pressure of extrusion	Adequate	Very high	High	Adequate	Adequate
Extrudability	Adequate	*Not possible*	Poor	Excellent	Excellent
Buildability	Layer kneading	*Not possible*	Good*	Excellent	Excellent
Final result	Printed	Not printed	Partially printed	Printed	Printed
Finishing	Average	*Not possible*	Good**	Excellent	Very good

** The quality of mortar is good, but as the pressure extrusion is too high, the piece was not completely printed due to the limitation of equipment; ** evaluating the piece printed*

The reference composition enabled the completion of the printing process, as it is the material recommended by the manufacturer for the equipment utilized. However, noticeable kneading of the lower layers was observed, and the finish achieved upon completion of printing was deemed unsatisfactory. A minor phase separation occurred during printing, with free water becoming visible on the surface of the printed cylinder. All compositions exhibited satisfactory fluidity and pumpability. However, Mix 1 encountered significant difficulty in extruding from the nozzle of the extruder. Consequently, printing was not feasible as it surpassed the machine's torque limit. Mix 2 also faced nozzle exit issues, but printing started, nonetheless. However, after approximately 10 cm of height, the process was halted due to reaching the machine's torque limit. Nevertheless, despite these challenges, a satisfactory final finish was achieved, and the printed layer thickness was maintained. On the other hand, Mix 3 and Mix 4 compositions allowed for the complete printing of the piece with excellent finishes, with Mix 3 being deemed more suitable.

From the qualitative assessment, certain trends were observed, and by incorporating rheological evaluation, we aimed to gain insights into the results obtained during the printing

https://doi.org/10.24355/dbbs.084-202408160950-0

process. Fig. 2 illustrates the mixing stage of the mortars (on the left) and the rheological profile obtained by applying shear cycle rheometry (on the right). Table 4 summarizes the most relevant information about both tests below.

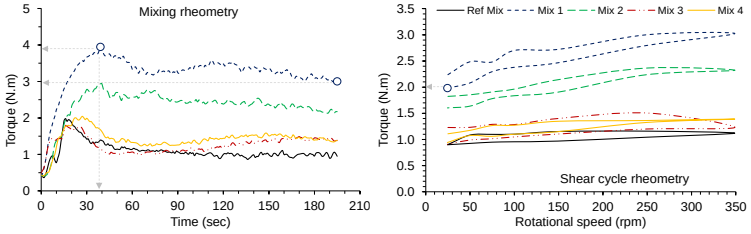

Fig. 2. Mixing rheometry (on the left) and rheological profile of compositions (on the right) obtained by applying shear cycle rheometry. On the left, the first circle represents the turning point, and the vertical arrow indicates the time to achieve it. At the end of the curve, the circle represents the final torque of mixing. On the right, the circle represents the yield torque.

Table 4. Maximum torque of mixing and time to achieve it, final torque of mixing, and energy required to mix, obtained during the test of mixing rheology. Yield torque end rheological behavior was obtained by applying the stepped flow test.

Property	Ref Mix	Mix 1	Mix 2	Mix 3	Mix 4
Maximum torque of mixing (N.m)	1.98	3.95	2.94	1.79	2.04
Time to achieve the maximum torque (sec)	16	39	40	19	27
Final torque (N.m)	0.90	3.07	2.19	1.45	1.37
Mixing energy (N.m/sec)	214	629	456	247	279
Yield torque (N.m)	0.90	1.98	1.60	0.91	0.94
Rheological behavior	Shear thinning	Shear thinning	Shear thinning	Shear thinning	Shear thinning

The first thing to be mentioned is that the mixing and application of the shear cycle test on the reference composition (Ref Mix) resulted in initial rheological patterns of the mortars. From the moment water comes into contact with the powder to initiate mixing, agglomeration forces intensify, rapidly increasing torque until reaching a maximum value. This torque value deserves attention because it represents the point of maximum cohesion of the mortar during mixing and is known as the turning point. Additionally, the time to reach this point in the mixture is also relevant, as the earlier this occurs, the more indicative it is of the onset of mixture fluidity. The final torque, conversely, may be correlated with the consistency of the mortar during the final mixing stage, while the mixing energy denotes the effort needed to produce the mass. In the instance of the reference mix, a low turning torque was observed, occurring in only approximately 16 seconds, along with low mixing energy, suggesting that the mix was easy to produce and that will not require more robust equipment. Mix 1, on the other hand, proved to be very difficult to mix, reaching the highest torque at the turning point, reached at the longest time, and the highest mixing energy, contrasting with the desired standard observed in the reference. Mix 2 also exhibited greater processing difficulty, while the other compositions (Mix 3 and 4) behaved similarly to the reference during mixing. All the mortars demonstrated shear thinning behavior, indicating suitability for pumping, and the yield torque of the Ref Mix, Mix 3, and Mix 4 were

https://doi.org/10.24355/dbbs.084-202408160950-0

similar. However, for Mix 1 and Mix 2, the minimum torque required to initiate flow was higher, potentially indicating difficulty for printing with low-power equipment.

Purely for illustrative purposes, Fig. 3 displays the flow results of the mortars obtained from the flow table test. Despite, no rheological information was obtained using this method, it was possible to observe that Mix 1 and 2 presented low spread, while Ref Mix, Mix 3 and 4 presented similarities, corroborating with results of yield torque. This test was just performed to show the adequate flowability, without phase segregation.

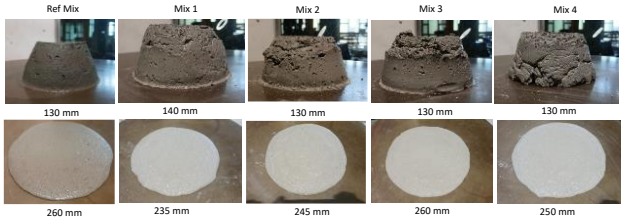

Fig. 3. Fluidity of mortars by flow table. Even though they showed good cohesion after removing the mold, the mortars spread a lot and homogeneously after the successive impacts.

To complement this analysis, the Benbow and Bridgwater test was performed, resulting in the graph presented in Fig. 4, correlating the extrusion pressure with the displacement. The extrusion profile of the reference composition was the most critical of all the compositions evaluated, indicating that this mix would require machines with greater power to print the product. In this case, the product formulated using only sand and cement resulted in a composition with high packing porosity of the aggregates and fines, with the highest volume of voids in both cases, but with a lower volumetric surface area, i.e. less water was needed to cover the finer particles, but the amount of water remaining to separate the particles and lubricate the aggregates was inefficient, generating phase separation during the process. As a consequence, the extrusion pressure increases intensely with small compressive deformations. The picture on the left side of the curve highlights the water remaining in the cup after the B&B test for this composition. This composition represents the standard specified by the company supplying the printing equipment, and it was possible to use it in printability tests. However, despite showing a shear thinning behavior and low torque after the end of the mixture, which also indicates, in this case, lower apparent viscosity, the profile obtained applying the B&B extrusion test is not recommended for good practice, That is, in a confined place, the movement of the mass was not adequate.

Fig. 5 illustrates the spreading of mortars using the squeeze flow test, correlation with the printability of compositions. In theory, the profile shows that the squeezed materials follow three main stages. The first is characterized by a linear elastic behavior with a small displacement [12]. The second is characterized by a plastic deformation or viscous flow where the material deforms considerably. The third stage is characterized by a strain-hardening behavior where the deformation growth rate decreases. All of the compositions evaluated presented both stages but with different intensities of load in the function of displacement. This means that for the same spread, the compositions respond with distinct printability. Comparing only Mixes 3 and 4, no considerable differences were observed up to around 90% of displacement. Displacements higher than this percentage indicate the

https://doi.org/10.24355/dbbs.084-202408160950-0

beginning of the strain hardening stage on Mix 4. On the other hand, the other compositions (mixes Ref, 1 and 2) presented higher compressive load since the beginning of the test, representing considerable difficulty to start the flow. In addition, the quick rise in the load illustrates that would not be possible to print layers with a large spread, limiting the buildability and the growth of piece. For instance, at the beginning of the spread (i.e.: 20%) the compressive load was 4 times higher than for Mixes 3 and 4, and was intensified with by squeezing the sample, differentiate them, considerably.

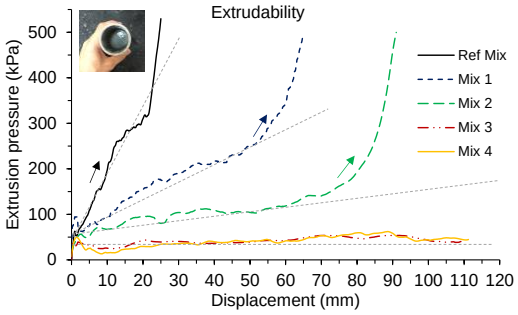

Fig. 4. Extrusion pressure of mortars according to the Benbow and Bridgwater test.

Thus, the SF test can illustrate that the thickness of the layer during printing must be limited, i.e. the crushing of the layer must only occur during the viscous regime, with the maximum dimension immediately before the start of strain hardening.

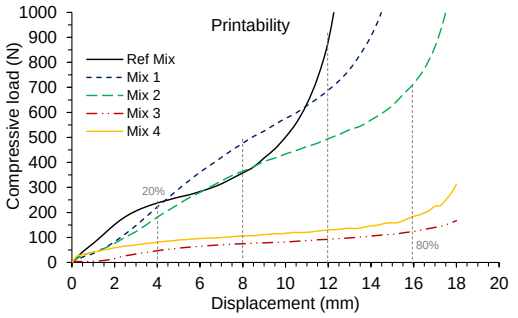

Fig. 5. Spreading of the mortars from a squeeze flow test.

By the end, a survey did by *Pan* [8] analyzing more than 150 papers published worldwide from 2016 and 2022, illustrated that the Portland cement consumption in compositions for 3D-printing ranged from 310 to 2,015 kg/m³, with an average of 1,074 kg/m³. The minimum value was observed in compositions of cellular concrete, i.e., around 80% of voids. The results obtained in this present study were 639 kg/m³ in the reference composition and 288 kg/m³ in the other compositions developed, i.e., the products developed in this study (except for the Ref Mix suggested by the producer of 3D printer) present consumption below the minimum values observed worldwide, with very good properties on the fresh state, representing adequate printability. So, the strategy used in this study can be useful for the development of eco-friendly compositions for 3D-printing.

https://doi.org/10.24355/dbbs.084-202408160950-0

6 Conclusions

The development of eco-efficient compositions for 3D printing, inevitably, involves the proper choice of rheological methods to represent each stage of the process. A reference composition recommended by the equipment manufacturer was used as a rheological reference. In this case, the binder consumption was high, however, the printing was carried out successfully (although the finish was not of good quality). A summary of the main qualitative parameters observed during printing was presented as a way of comparing the compositions, emphasizing the pumpability and flowability of the compositions, the initial pressure demand for the nozzle exit, the potential for extrusion and buildability, and the aspects related to the quality of the printed product. Of the 5 compositions evaluated, although all had adequate pumpability, only 3 were printed until the end (Ref Mix, Mix 3 and Mix 4). One of them was not printed completely, as it exceeded the torque limit of the equipment (Mix 1), and one of them could not be printed (Mix 2). From the application of rheological tools, was possible to understand each characteristic of the products. All compositions showed shear thinning behavior, suitable for pumping, in the same way, that all presented similar flowability according to the flow table test. However, from the squeeze flow and Benbow and Bridgwater tests, different extrusion pressures and viscous flow of the materials were found. Thus, it can be proven that the compositions with the better rheological properties (Mix 3 and Mix 4) were the ones that presented greater ease of printing and better finishing of the products. At the end of the paper was presented a survey illustrating a global scenario of binder consumption in the compositions referenced worldwide and the positioning of the compositions developed in our world using the strategy proposed.

References

1. Buswell RA, Leal de Silva WR, Jones SZ, Dirrenberger J. 3D printing using concrete extrusion: A roadmap for research. Cement and Concrete Research 2018;112:37–49.
2. Wangler T, Lloret E, Reiter L, Hack N, Gramazio F, Kohler M, et al. Digital Concrete: Opportunities and Challenges. RILEM Technical Letters 2016;1:67–75.
3. Klyuev S, Klyuev A, Fediuk R, Ageeva M, Fomina E, Amran M, et al. Fresh and mechanical properties of low-cement mortars for 3D printing. Construction and Building Materials 2022;338:127644.
4. John VM, Damineli BL, Quattrone M, Pileggi RG. Fillers in cementitious materials — Experience, recent advances and future potential. Cement and Concrete Research 2018;114:65–78.
5. Han F, Pu S, Zhou Y, Zhang H, Zhang Z. Effect of ultrafine mineral admixtures on the rheological properties of fresh cement paste: A review. Journal of Building Engineering 2022;51:104313.
6. Al-Noaimat YA, Chougan M, Al-kheetan MJ, Al-Mandhari O, Al-Saidi W, Al-Maqbali M, et al. 3D printing of limestone-calcined clay cement: A review of its potential implementation in the construction industry. Results in Engineering 2023;18:101115.
7. Jeong H, Han SJ, Choi SH, Lee YJ, Yi ST, Kim KS. Rheological Property Criteria for Buildable 3D Printing Concrete. Materials 2019;12:657.
8. Pan EM. Análise do cenário atual de desenvolvimento da tecnologia de manufatura aditiva com composições cimentícias aplicadas a construção civil. 2024.
9. De Schutter G, Lesage K, Mechtcherine V, Nerella VN, Habert G, Agusti-Juan I. Vision of 3D printing with concrete — Technical, economic and environmental potentials. Cement and Concrete Research 2018;112:25–36.

https://doi.org/10.24355/dbbs.084-202408160950-0

10. Westman AER, Hugill HR. THE PACKING OF PARTICLES1. J American Ceramic Society 1930;13:767–79.
11. Benbow JJ, Bridgwater J. The cutting of paste extrudates. Chemical Engineering Science 1993;48:3088–91.
12. Grandes FA, Sakano VK, Rego ACA, Cardoso FA, Pileggi RG. Squeeze flow coupled with dynamic pressure mapping for the rheological evaluation of cement-based mortars. Cement and Concrete Composites 2018;92:18–35.

https://doi.org/10.24355/dbbs.084-202408160950-0